Ultrasonics Sonochemistry 112 (2025) 107151

Contents lists available at ScienceDirect

Ultrasonics Sonochemistry

journal homepage: www.elsevier.com/locate/ultson

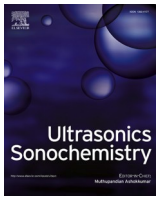

Effect of ultrasound combined with plasma protein treatment on the structure, physicochemical and rheological properties of myofibrillar protein

Ye Zou [a,b], Lingjuan Wang [a,b], Xiaowen Wang [a,b], Yibo Lan [a], Jingjing Ma [a], Jing Yang [a], Weimin Xu [a,b], Qi Shen [a,b,*], Daoying Wang [a,b,*]

[a] Institute of Agricultural Products Processing, Jiangsu Academy of Agricultural Sciences, Nanjing 210014, China
[b] School of Food and Biological Engineering, Jiangsu University, 301 Xuefu Rd., 212013 Zhenjiang, Jiangsu, China

ARTICLE INFO

Keywords:
Ultrasound treatment
Plasma protein
Myofibrillar protein
Gumminess
Rheological property

ABSTRACT

This study aimed to investigate the effect of ultrasound combined with plasma protein (UPP) treatment on the structure, physicochemical and rheological properties of myofibrillar protein (MP). The results indicated that the UPP group caused changes in the secondary structure, increased fluorescence intensity and enhanced surface hydrophobicity of MP. Then, UPP significantly decreased the content of free and total sulfhydryl group, and high molecular weight protein contents were observed in MP. These findings implied moderate cross-linking and aggregation between plasma protein and MP in this ultrasound treatment. Furthermore, the physical characteristics, stability and rheological properties of MP were improved in UPP, as evidenced by increased storage modulus and decreased loss angle tangent. Therefore, this study suggested that the combined treatment not only had the potential to enhance the product quality in the process of ground meat, but also improved the utilization rate and added value of plasma proteins.

1. Introduction

Meat, which contains proteins, fatty acids, trace elements and vitamins, is a crucial energy source for human growth and development. It plays an essential role in global food security, nutrition and health [1]. During the slaughter and processing of meat products, a small amount of ground meat is produced. Taking broiler chickens as an example, the proportion of ground meat is 1.86 %. The total global broiler production in 2023 is 102.389 million tons [2]. Therefore, the total amount of ground meat is also considerable. It is interesting to deep process ground meat into high value-added products. Ground meat is commonly used in meat product production and requires additional additives to improve its quality [3,4]. Plasma proteins, obtained from animal plasma through methods as spraying or freeze-drying, comprise a range of biologicially active components including peptides, immunoglobulins and superoxide dismutase. This has earned themas the nickname “liquid meat” [5]. The high nutritional value and binding properties make them promising natural food additive [6]. According to Hurtado et al. [7], plasma protein could enhance the quality characteristics of minced pork, comparable to soybean protein and casein except for hardness, while also increasing product yield.

Ultrasound treatment had widely utilized as auxiliary processing method in meat industry to enhance the quality of the meat products [8]. Particularly, the effectiveness in tenderizing meat has been extensively demonstrated and applied. For instance, Xiong et al. [9] reported that ultrasonic-assisted curing could enhance chicken tenderness and increase the water holding capacity. In addition, myofibrillar protein (MP), which accounted for approximately 50 ~ 60 % of total muscle protein and played a crucial functional role in meat processing [10], could be significantly affected by ultrasound. The cavitation effect and other mechanical effects produced by ultrasound altered the forces maintaining the MP structure, leading to unfolding in tertiary structure and the changes in secondary and quaternary structure [11]. These modifications reduced aggregation degree and improved solubility of MP. The resulting alterations were advantageous for the formation of a uniform gel network, which improve the water holding capability and structural strength of sausages and other minced meat products [12].

In a previous study, the combination of ultrasound assisted plasma

* Corresponding authors at: Institute of Agricultural Products Processing, Jiangsu Academy of Agricultural Sciences, Nanjing 210014, China.
E-mail addresses: jaas2008@163.com (Q. Shen), daoyingwang@yahoo.com (D. Wang).

https://doi.org/10.1016/j.ultsonch.2024.107151
Received 10 October 2024; Received in revised form 29 October 2024; Accepted 8 November 2024
Available online 9 November 2024

protein in ground meat were utilized to produce chicken patties. It addressed the issue of increased patty hardness when using plasma protein as an adhesive [13]. However, the role at the molecular level behind these positive effects of the combined treatment has not been elucidated. Therefore, this study aimed to investigate the impact of ultrasound combined with plasma protein treatment on the structure, physicochemical and rheological properties of MP.

2. Materials and methods

2.1. Materials

The ground chicken meats were purchased at Jiangsu Lihua Animal Husbandry Co., Ltd (Changzhou, China) and stored at 4 °C after removing the connective tissue and fascia. The plasma protein powder, with the purity of 70 %, was provided by Qinhuangdao Jinhai Food Co., Ltd. All other reagents used in the experiment were of analytical grade.

2.2. Extraction of MP

The MP extraction method was adjusted based on the research studies by Jiang et al. [14]. Briefly, raw minced meat was mixed with precooled buffer solution A (0.1 M NaCl, 2 mM $MgCl_2$, 1 mM EGTA, 10 mM Na_2HPO_4/NaH_2PO_4, pH 7.0) at a ratio of 1:4 (v/v). The mixture was then homogenized in an ice-water bath at 10000 rpm for 60 s and subsequently centrifuged for 15 min (2000 × *g*, 4 °C), repeated three times. After that, the precipitate was added to precooled buffer solution B (0.1 M NaCl, pH 6.25) at a ratio of 1:8 (v/v) before being homogenized and centrifuged three times under the same conditions as described above. After the third homogenization, the suspension was filtered through four layers of gauze. The MP obtained was precipitated in 15 mM PIPES buffer (1, 4-piperazine-N, N-(2-ethanesulfonic acid), pH 6.25, containing 0.6 M NaCl) and stored in a refrigerator at 4 °C for use within 72 h. The concentration of MP was determined using the biuret method.

2.3. Preparation of composite protein system

The MP solution was adjusted to a concentration of 10 mg/mL using PIPES buffer. Following centrifugation at 500 × *g* for 5 min to remove air bubbles, this solution was designated as the mother solution. The untreated solution was labeled as MP. In the PP group, plasma protein was added at 15 % (w/w) of the MP mass in the mother solution. Subsequently, fixed volumes (100 mL) of both MP and PP solutions were subjected to ultrasound treatment, resulting in UMP and UPP, respectively. Ultrasound was applied using a JY 92-IIN ultrasound processor (Ningbo Xinzhi Instrument Co., Ltd.) equipped with a 6 mm diameter probe, immersed in an ice water bath for 9 min (190 W, with sonication occurring every 2 s followed by a 3 s pause).

2.4. SDS/Native-PAGE

SDS/Native-PAGE was conducted following the protocol described by Jiang et al. [14] with minor adjustments. Electrophoresis was carried out at 150 V for both techniques. The reagents utilized for Native-PAGE were identical to those for SDS-PAGE, except for the electrophoresis buffer (0.05 M Tris-0.384 M glycine, pH 8.3) and the loading buffer (omitting β-mercaptoethanol). Importantly, protein samples were not subjected to heat treatment during Native-PAGE. Subsequently, the electrophoretic patterns were captured using a Charge-Coupled Device camera (Raytest, Camilla II, Straubenhardt, Germany), and the gray-scale distribution of protein bands was analyzed using Image J software.

2.5. FTIR spectroscopy

The FTIR spectra of the samples were acquired using a Fourier transform infrared spectrometer (Nicolet iS50, Thermo Fisher, USA). Each complex protein solution (approximately 200 μL) was deposited onto the sample stage. The probe height was adjusted to 2 mm above the stage, and the FT-IR spectra were measured over the range of 4000 ~ 400 cm^{-1} with a scanning accumulation of 64 times at an ambient temperature of 25 ± 0.2 °C. The amide I band (1700 ~ 1600 cm^{-1}) was subjected to deconvolution and Gaussian fit using the Peak Fit Version 4.12 software with reference to the method of Li et al. [15]. This approach facilitated the determination of the relative content of secondary structures across different treatment groups.

2.6. Intrinsic and synchronized fluorescence spectroscopy

The four groups of complex protein system solutions were diluted 50-fold before being placed in a fluorescence analyzer (F-7000, Hitachi Co., Tokyo, Japan). The intrinsic fluorescence spectra were measured at an excitation wavelength of 280 nm and a scanning range of 285 ~ 420 nm. Additionally, the synchronized fluorescence spectra of tyrosine (Tyr, Δλ = 15 nm, scanning range of 260 ~ 320 nm) and tryptophan (Typ, Δλ = 60 nm, scanning range of 220 ~ 320 nm) were measured separately. Spectral scans were conducted with a slit width of 3 nm and a scan rate of 600 nm/min.

2.7. Surface hydrophobicity

The method of Chen et al. [16] was referenced and slightly modified for the determination of surface hydrophobicity. Specifically, each of the four complex protein systems was diluted 2-fold in PIPES buffer (15 mM, pH 6.25). Following dilution, the diluted samples (2 mL) was mixed with 20 μL of 8-Anilino-1-naphthalenesulfonic Acid (ANS, 8 mM) and allowed to stand for 20 min at 4 °C in dark. Subsequently, the fluorescence intensity of the reaction mixture was measured using a fluorescence spectrophotometer, with excitation at 390 nm and emission detection at 470 nm. The spectrophotometer settings included a slit width of 3.0 nm and a scanning frequency of 3 times.

2.8. Determination of total sulfhydryl content and active sulfhydryl content

Total sulfhydryl and active sulfhydryl content were determined according to the slightly modified method of Zhao et al. [17]. For the measurement of reactive sulfhydryl content, the complex protein solution system was diluted 25-fold with 15 mM PIPES buffer (10 mM EDTA, pH 7.5). Each 5 mL sample was mixed with 0.5 mL of DTNB (0.2 % w/w in 15 mM PIPES, pH 7.5) and incubated at 4 °C for 1 h. The absorbance value at 412 nm (A_{412}) of the resulting mixture was measured using a microplate spectrophotometer (Multiskan SkyHigh, Thermo Scientific, USA). For the determination of total sulfhydryl content, the diluent used was 15 mM PIPES buffer (10 mM EDTA, pH 7.5) containing 8 M urea, and the other conditions were described as above.

2.9. Zeta potential and particle size

The solutions were diluted 10-fold and 100-fold with PIPES buffer, respectively, and an appropriate volume of each diluted was taken to measure the zeta potential and particle size using the Nano-ZS90 nano-laser particle sizer. For particle size measurement, sample solution (1.5 mL) was injected into a clean quartz cuvette with an optical diameter of 1 cm. The average particle size (Z-average) and particle size distribution of each sample were measured and recorded.

2.10. Rheological properties

The rheological properties of the samples were evaluated using a hybrid rheometer (Discovery HR10), following the method described by Chen et al. [16] with some modifications. Both static and dynamic rheological properties were measured using a 60 mm parallel plate. An

appropriate amount of sample was aspirated onto a sample stage equipped with circulating chilled water refrigeration system to maintain a temperature of 25 ± 0.2 °C. Frequency sweeps were performed at a fixed 5 % shear strain, with the shear rate ranging from 0.1 to 100 s^{-1}. The changes in apparent viscosity, storage modulus (G′) and loss modulus (G″) with shear rate were recorded, and the loss tangent was calculated:

$$\tan\delta = \frac{G''}{G'}$$

2.11. Data analysis

Three parallels were set up for each experiment, and the experimental data were statistically analyzed using SPSS 27 (IBM, Chicago, USA). The data were expressed as mean ± standard deviation and Duncan's multiple-comparison was conducted to evaluate differences at the level of $P < 0.05$.

3. Results and discussion

3.1. SDS/Native-PAGE

Native-PAGE provides a comprehensive view of protein molecular weight distribution and illustrates the position of cross-linked products. This result was instrumental in elucidating the cross-linking mechanism between MP and plasma protein (Fig. 1). As displayed in Fig. 1A, the bands of Native-PAGE were segmented into three sections and normalized in Fig. 1B. These results revealed that the ultrasound treatment facilitated the modification of MP (UMP). Additionally, the introduction of plasma protein led to the formation of a polymer cross-linking complex involving the myosin heavy chain (MHC) in PP. The amount of cross-linked product increased significantly due to the synergistic effect of ultrasound assisted plasma protein treatment (UPP). This enhancement was directly reflected in the relative content of high molecular weight segment, with a decrease observed in myosin heavy chain (MHC) in UMP compared to MP. Conversely, the relative content of dissociation products from MPs corresponding to the low molecular weight segment increased accordingly. These results suggested that ultrasound treatment could disrupt the forces maintaining spatial structure of MPs, leading to dissociation [14,16]. However, the content of MHC decreased as the relative gray ratio of the high molecular weight segment significantly increased ($P < 0.05$) under the combined influence of ultrasound and plasma protein. This indicated that the formation of high molecular weight polymers resulting from the cross-linking of plasma protein with MHC. In addition, there were no significant difference in the number and depth of bands in the protein systems, particularly for MHC and actin, which exhibited high optical density (Fig. 1C). Thus, ultrasound treatment and the addition of plasma protein did not alter the subunit compositions of the protein systems. The formation of polymerization polymerization products was mainly predominantly driven by disulfide bonds, which consistent with the findings reported by Gao et al. [18].

3.2. FTIR characterization

FTIR spectroscopy is a powerful tool for examining interactions and local environments of functional groups within protein side chains. The absorption peaks within the amide I band (1600 ~ 1700 cm^{-1}), II band (1500 ~ 1600 cm^{-1}), and III band (1220 ~ 1330 cm^{-1}) were mainly caused by C═O stretching vibration, N–H bending vibration, and C–N stretching vibration, respectively (Jiang et al., 2018). The spectra of the amide I band region could be deconvoluted and fitted with the second-order derivative to determine the relative content of four secondary structures (Fig. 2A and B, 1650 ~ 1658 cm^{-1} of α-helix, 1610 ~ 1640 cm^{-1} of β-sheet, 1660 ~ 1700 cm^{-1} of β-turn and 1640 ~ 1650 cm^{-1} of random coil) [20].

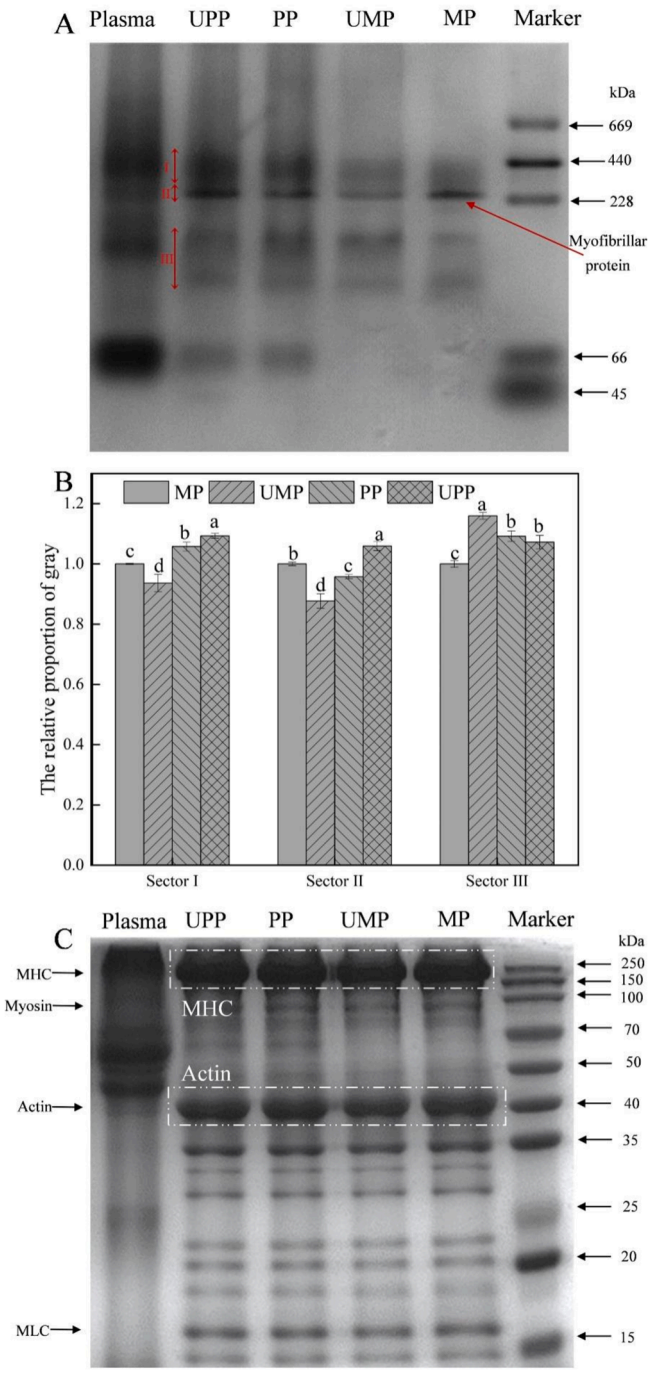

Fig. 1. Gel electrophoresis results of MP (myofibrillar protein), UMP (ultrasound combined with myofibrillar protein), PP (plasma protein) and UPP (ultrasound combined with plasma protein). (A) Native-PAGE result of different treatments. (B) The relative proportion of different sectors in different treatments. (C) The SDS-PAGE result of different treatments. Error bars indicate the standard errors of the mean. Different lowercase letters represent the significance ($P < 0.05$) among different groups under the same sector.

As shown in Fig. 2C, the UMP group displayed a reduction in the percentage of α-helix and random coil, accompanied by an increase in the total percentage of β-sheet and β-turn compared to the MP group. A similar trend was observed in the UPP group compared to the PP group, indicating that the protein structure of the composite protein system tended to unfold after ultrasound treatment combined with plasma protein. This observation aligns with findings by Zhao et al. [17], who noted that ultrasound treatment can decrease the relative content of

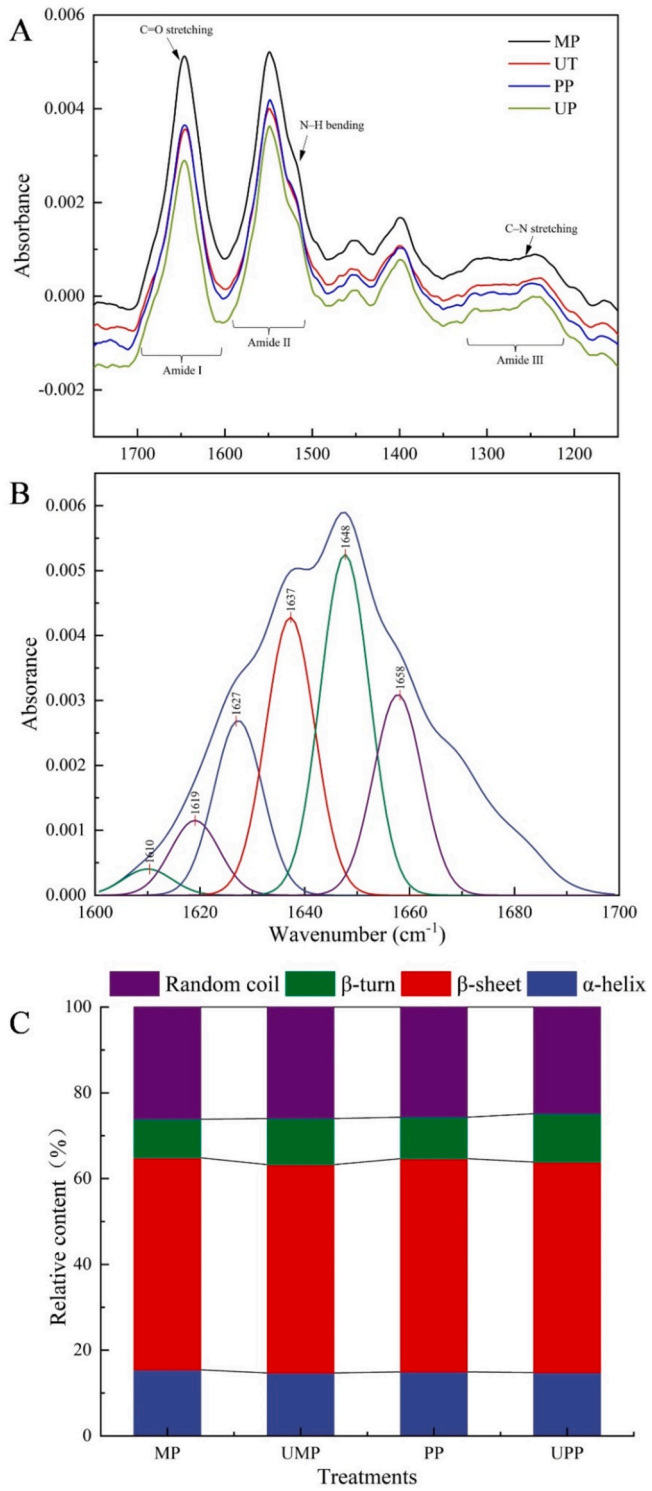

Fig. 2. The secondary structure property of different groups. (A) FTIR spectroscopy of different treatments. (B) An example of Gaussian fit (MP). (C) Relative content of the secondary structure in different groups.

α-helical structures while increasing the proportion of β-sheet. In general, α-helices mainly formed due to the driving action of intermolecular hydrogen bonding within the protein molecule [19]. Transitioning from α-helices and random coil to β-sheet involves breaking intermolecular hydrogen bonds, thereby exposing functional groups originally contained within the proteins. The β-sheet structure, characterized by a large surface area and weak hydration strength, is conducive to cross-linking between protein molecules [18]. This structural transformation also correlated with changes observed in sulfhydryl groups across different treatment groups.

3.3. Fluorescence characterization

Proteins could exhibit intrinsic fluorescence upon excitation at 280 nm, attributed to the presence of aromatic amino acids. The fluorescence property is sensitive to microenvironment changes, making intrinsic fluorescence spectra a valuable tool for evaluating alterations in the tertiary structure of proteins [21]. Furthermore, the synchronous fluorescence spectra with a wavelength difference of 15 nm and 60 nm could provide insights into microenvironmental properties of tyrosine (Tyr) and tryptophan (Typ), respectively.

As shown in Fig. 3A, the fluorescence intensity of the PP group was the largest at the same dilution, followed by that of the UPP group. This indicated that both ultrasound treatment and the addition of plasma protein led to increased intrinsic fluorescence values compared to the untreated MP. The ultrasound treatment unfolded proteins, exposing aromatic amino acid groups that were originally embedded in the hydrophobic center of the protein to a polar environment [22]. The maximum emission wavelength (λ_{max}) shifted from 333.5 nm in the MP to 334.5 nm in the UMP and 334 nm in the UPP (Table 1), reflecting an increase in the polarity of the microenvironments [23]. Although fluorescence intensity (FI) increased with higher protein concentration after adding plasma proteins, λ_{max} was not influenced. However, the FI of UPP was lower than that of the PP group but higher than that of MP group. Jiang et al. [14] also discovered that ultrasound diminished the FI of proteins due to the cavitation effect and microtreaming. These phenomena promoted collisions and interactions among protein molecules and residues, resulting in the embedding of initially unexposed aromatic amino acids into the cross-linked proteins through π-π stacking. Consequently, FI decreased and a blue shift occurred [17]. The results showed that UPP induced partial expansion and contraction in the tertiary structure of the protein system. This effect was found more complex and significant in cross-linking with plasma protein. The synchronized fluorescence spectra depicted in Fig. 3B and C exhibited fluorescence properties and trends similar to those observed in the intrinsic fluorescence spectra. However, the results clearly indicated that the tryptophan residues were the primary contributors to these fluorescence properties. This was evident as the fluorescence of Typ did not exhibit significant change in response to the microenvironment, whereas the fluorescence properties of proteins were typically dominated by Tyr.

3.4. Surface hydrophobicity analysis

ANS is an anionic fluorescent probe known for its selective binding to non-polar regions of proteins. The alteration in FI induced by ANS binding might reflect changes in the protein surface hydrophobicity. Fig. 3D indicated that the FI of the protein system in the UMP, PP, and UPP treatment groups gradually increased, showing enhanced surface hydrophobicity compared to the MP group ($P < 0.05$). This phenomenon was related to the exposure of non-polar groups and hydrophobic amino acids within the interior of proteins, induced by ultrasound treatment. This process facilitated the unfolding of the protein's spatial structure and the depolymerization of the side chain [24,25], which was consistent with the findings of Zhao et al. [17]. Furthermore, the addition of plasma protein also increased the surface hydrophobicity of the protein system. This was likely due to plasma protein containing more ANS binding sites, encompassing non-polar structural domains and hydrophobic amino acid residues [26]. Thus, the surface hydrophobicity of the UPP group was significantly enhanced compared to that of the MP group, attributable to the synergistic effect of ultrasound treatment and the addition of plasma proteins ($P < 0.05$). This indicated that the intermolecular interaction between MP and plasma protein was increased by ultrasound treatment.

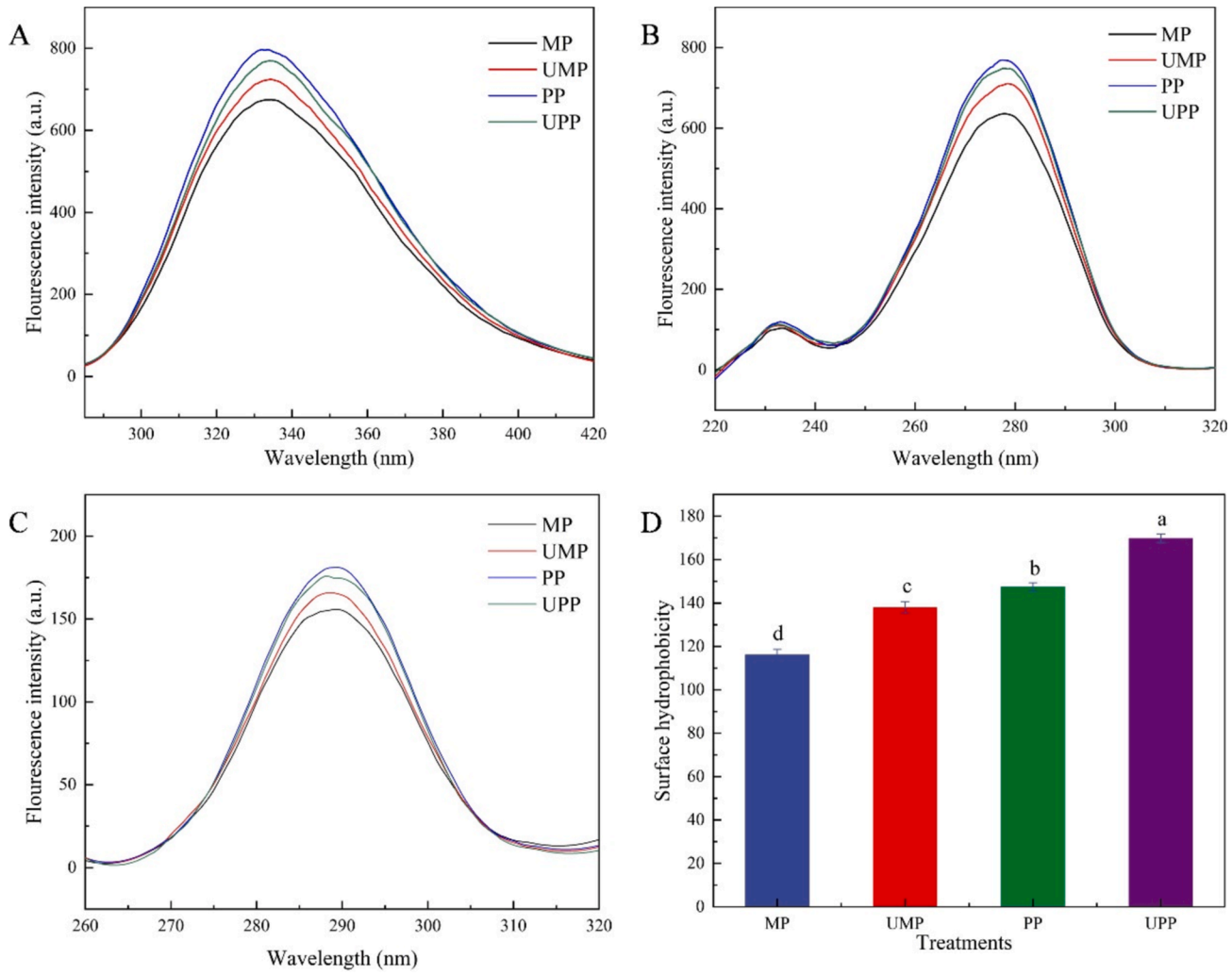

Fig. 3. The tertiary structure property of different groups. (A) Intrinsic fluorescence spectroscopy of different treatments. (B) Try fluorescence spectroscopy of different treatments. (C) Typ fluorescence spectroscopy of different treatments. (D) Surface hydrophobicity in different groups. Different lowercase letters indicate significant difference in each treatment ($P < 0.05$).

Table 1
The position of λmax in MP (myofibrillar protein), UMP (ultrasound combined with myofibrillar protein), PP (plasma protein) and UPP (ultrasound combined with plasma protein).

	Intrinsic fluorescence	Tyr	Typ
MP	333.5 nm	278 nm	289.5 nm
UMP	334.5 nm	278.5 nm	289.5 nm
PP	333.5 nm	278 nm	289.5 nm
UPP	334 nm	278 nm	289.5 nm

3.5. Analysis of total and free sulfhydryl groups constitute

Sulfhydryl groups in cysteine are prone to oxidation, forming disulfide bonds crucial for maintaining protein structural stability [27]. The Ellman method was used to determine the total and free sulfhydryl groups contents in the protein system obtained from different treatments. The results showed a significant reduction ($P < 0.05$) in both typs of sulfhydryl groups following ultrasound treatment (Fig. 4A). Specifically, the UMP group showed an 11.17 % decrease in free sulfhydryl groups compared to the MP group (600.87 ± 6.22 mmol/L), while the UPP group exhibited a decrease of 2.69 % compared to the PP group (535.53 ± 3.61 mmol/L). The UMP group demonstrated a 10.44 % decrease in total sulfhydryl content compared to the MP group (632.19 ± 4.38 mmol/L). Similarly, the UPP group exhibited a decrease of 6.24 % when compared to the PP group (565.48 ± 3.76 mmol/L). These changes were attributed to covalent cross-links between protein molecules, formed through oxidation of cysteine residues in the tail of myosin heavy chains [2]. This process resulted in the formation of disulfide bonds and a reduction in the content of both free and total sulfhydryl groups [28]. Additionally, based on the changes in sulfhydryl content observed in the UMP and PP groups compared to the MP group, it could be inferred that the intermolecular covalent cross-linking within the composite protein system could be strengthened by ultrasound and addition of plasma protein, respectively. On one hand, the spatial structure of protein was disrupted and expanded, rendering susceptibility of myosin and exposing a few reactive sulfhydryl groups. Moreover, the production of free radicals and microstreaming induced by ultrasound promotes the collision and oxidation of −SH groups [29,30]. On the other hand, plasma proteins might have the structural properties that facilitate their cross-linking with MPs, thereby promoting the formation of disulfide bonds that stabilize the protein structure. Thus, the reduction in sulfhydryl content was exacerbated in UPP group, which contributed to enhancing protein stability and resistance ($P < 0.05$). Zou et al. [31] also discovered that ultrasound could induce covalent cross-linking of konjac glucomannan with plasma proteins through disulfide bonds.

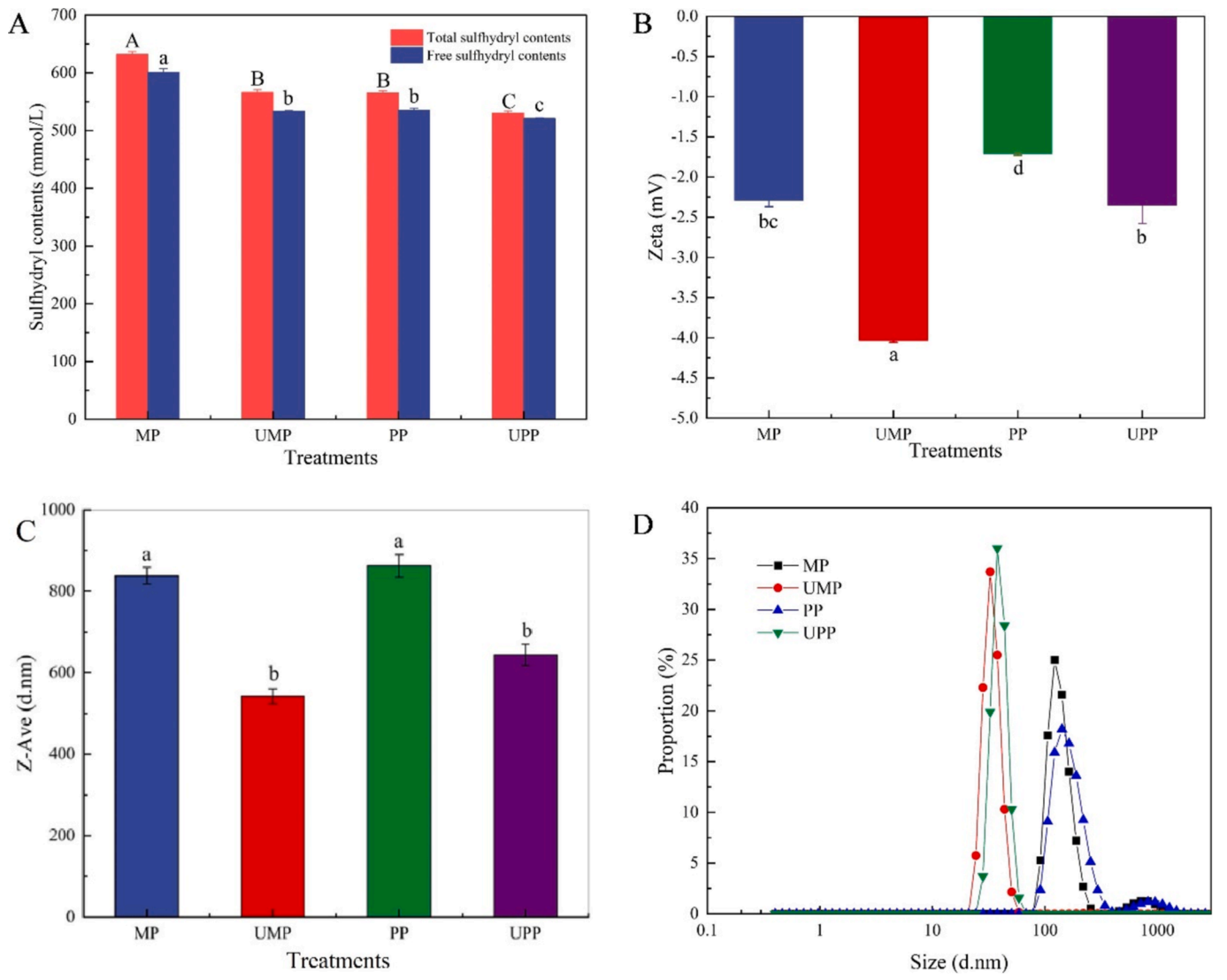

Fig. 4. The changes of sulfhydryl group content and physicochemical characters in different groups. (A) Total and free sulfhydryl group determinations in different groups. (B) Zeta potential in different groups. (C) Average particle size in different groups. (D) Particle size distribution in different groups. Different letters indicate significant difference in each treatment for each parameter ($P < 0.05$).

3.6. Zeta potential analysis

The zeta potential plays a critical role in the dispersion stability of the composite protein system, reflecting the strength of electrostatic interactions between protein molecules. The changes in zeta potential for each experimental group are illustrated in Fig. 4B. While all groups exhibited negative potentials, the absolute value of the potential significantly increased following ultrasound treatment. This increase in surface charge indicated structural modifications in the proteins, potentially exposing electronegative groups in specific amino acids ($P < 0.05$). As a result, the electrostatic interactions among protein molecules increased, thereby enhancing the stability of protein solutions. In addition, the addition of plasma protein significantly reduced the absolute value of the zeta potential of MP system (2.29 ± 0.078) by a decrease of 21.97 % ($P < 0.05$). This reduction could be attributed to the interaction between the positively charged groups in plasma protein and electronegative amino acid residues on the surface of MPs. Consequently, the electrostatic interactions within the composite protein system decreased, resulting in protein molecules aggregation and decreased solution stability [32]. Moreover, ultrasound cavitation affected the PP group by destroying weak interactions such as hydrogen bonding within protein molecules and enhancing the electronegativity of protein molecule. This, in turn, reduced the aggregation of plasma proteins and MPs, effectively improving the stability of the composite protein system. These findings aligned with the results of rheological properties to a certain extent (Fig. 4). Therefore, it was recommended to introduce ultrasound assisted plasma protein treatment to improve the MP stability.

3.7. Particle size analysis

The average particle size and particle size distribution could be used to assess the aggregation degree of protein molecules. Fig. 4C and D demonstrated the average particle size and distribution of the protein system in each treatment group, indicating that the various treatments had a noteworthy effect on them. The ultrasound treatment caused a leftward shift in the peak of the particle size distribution, narrowing the distribution width and significantly reducing the average particle size ($P < 0.05$). In contrast, the addition of plasma proteins to MPs resulted in a rightward shift of the peak position of the particle size distribution and an increase in the distribution width of protein system. The effect of ultrasound on protein particle size was consistent with the previous findings [16]. Coincidentally, Li et al. [15] also found that appropriate ultrasound power could reduce protein particle size. This reduction

might be attributed to the powerful disruptive force of ultrasound, which disrupted the electrostatic interactions, hydrogen bonding and other non-covalent forces among proteins. As a result, larger protein particles were depolymerized, forming fragmented structures, and decreasing in average particle size [16,28]. In addition, as shown in Fig. 4D, the peak position of the UPP group exhibited a rightward shift in the peak position comparison to the UMP group. These changes indicated that the combined treatment of ultrasound and plasma protein on MPs facilitated the cross-linking among proteins, leading to the formation of larger protein aggregates [30,33]. For these reasons, the microstreaming effect and shock waves generated during the ultrasound process might accelerate the movement of protein molecules within solutions. This increased the likehood of mutual collision between protein molecules and subsequently promoted the generation of weak intermolecular interaction forces, such as hydrogen bonding, which drove protein cross-linking. Consequently, the peak position in the particle size distribution shifted to the right.

3.8. Static rheological characterization

Static rheology could visually reveal the alternations in solution viscosity with shear rate, providing insights into the adhesive viscosity and flow characteristics of protein solutions under different treatment conditions. It also offered information on the strength of molecular interactions within the protein system [34,35]. As depicted in Fig. 5B, the viscosity of all four groups gradually climbed with shear rate, peaking at 0.1956 S^{-1} before decreased. In other words, the protein system exhibited shear thickening properties at low shear rates, transitioning to shear thinning as shear rates increase. Because of the significant spatial resistance effect and internal friction within MP, molecular cross-linking resistance of the system initially increased, resulting in an increase in viscosity. However, upon application of a shear force, the rod-like chain structure of MPs became oriented in the direction of the shear surface, causing a reduction in viscosity in the direction of flow [36]. At a maximum of 81.1585 S^{-1}, the MP, UMP, PP, and UPP groups exhibited viscosities of 0.1099, 0.1246, 0.1092, and 0.1437 Pas, respectively. Throughout the varying shear rate, the UPP group consistently demonstrated higher viscosity values compared to the other groups. This observation indicated that the combination treatment of ultrasound and plasma protein significantly enhanced the viscosity of the composite protein system. This enhancement might be likely due to the promotion of protein–protein interactions by the combined treatment of ultrasound and plasma proteins, leading to covalent cross-linking and rearrangement within the composite protein system [37]. As a result, more structurally stable biomolecules were formed, which improved the overall viscosity of the protein solution. Furthermore, in the study conducted by Chen et al. [16], ultrasound was similarly effective in promoting the covalent reaction among MPs, resulting in more stable protein solutions with improved viscosity.

3.9. Dynamic rheological characterization

The changes in storage modulus (G′) and loss modulus (G″) of the protein system under different treatment conditions were shown in Fig. 5A. It could be evident that the behavior of G′ and G″ was consistent across all experimental groups as the oscillation frequency ranged from 0.1 rad/s to 100 rad/s. Specifically, G′ exhibited a rapid increase followed by a gradual decrease, peaking at 39.81 rad/s in the PP group. Meanwhile, the value of G″ increased gradually at a relatively constant rate. However, in the other three groups, G′ consistently exceeded G″, except in the PP group where their intersection occurred at about 55 rad/s.

It was evident that G′ consistently surpassed G″ across the scanning frequency range, and G″ in the PP group was consistently lower compared to the other groups. This indicated that the MP, UMP, and UPP protein systems all exhibited viscoelastic solid properties [38].

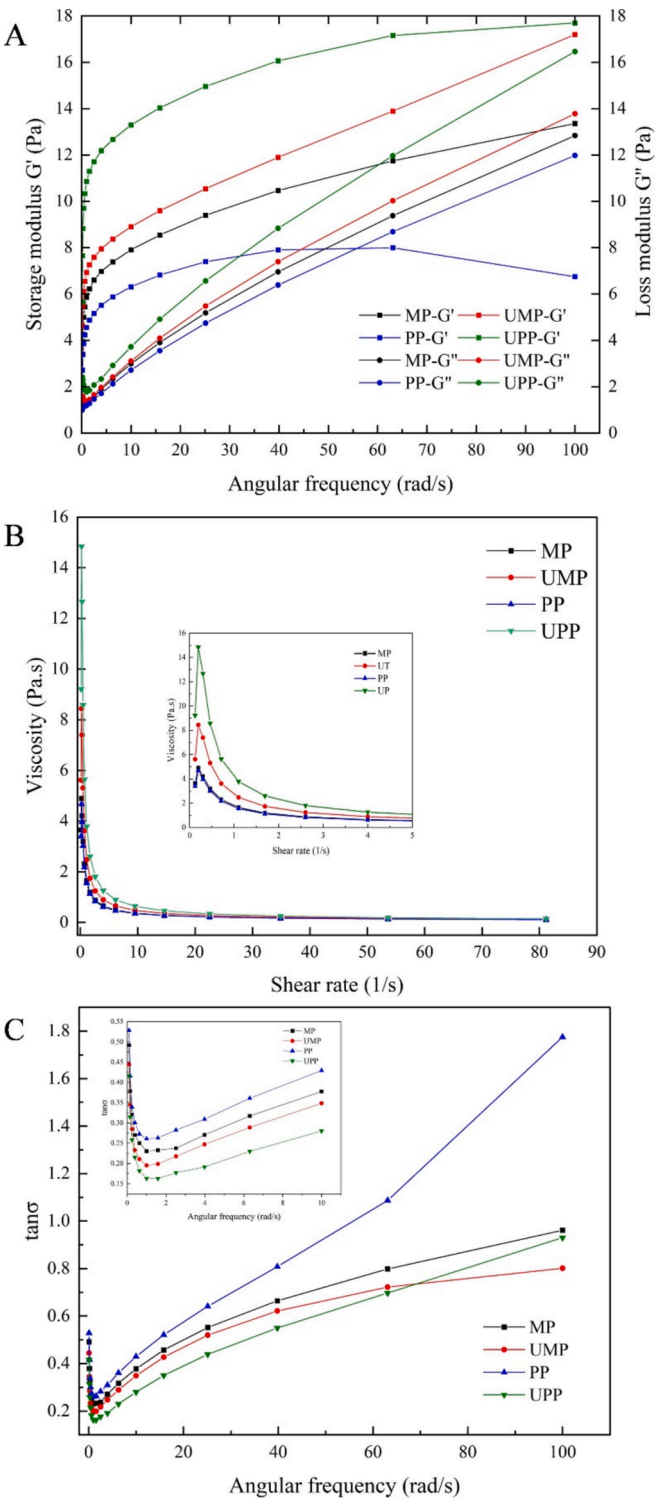

Fig. 5. The rheological characteristics of different groups. (A) Storage modulus and loss modulus in different groups. (B) Apparent viscosity in different groups. (C) Loss angle tangent in different groups.

However, in the PP group, a structural transition in the composite system occurred at the intersection point (tanδ = 1). At this point, the liquid-like properties began to dominate the structural characteristics of the PP group, leading to the gradual collapse of the composite system [39,40]. This phenomenon likely stemmed from the formation of a composite protein system where plasma proteins and MPs were primarily bound by weak intermolecular interactions, such as hydrogen

bonding, which are inherently less stable. However, the G′ and G″ of the UPP group were significantly higher compared to the other groups ($P < 0.05$), indicating that the combination of ultrasound and plasma proteins significantly enhanced the structural integrity of the composite protein system. The improvement observed in the composite protein system could be attributed to the synergistic interaction between ultrasound and plasma proteins. The interaction enhanced the covalent bonding, such as disulfide bonding, and improved the viscoelastic solidity of the solution [20]. The change could also be reflected in the Fig. 5C. The tanδ values for all samples, except the PP group, ranged between 0.1 and 1, indicating that all four composite protein systems exhibited typical weak gel properties rather than elastic gels (tanδ < 0.1). Among these groups, the UPP group demonstrated the lowest tanδ value at an oscillation frequency of approximately 70 rad/s, surpassing that of the UMP group. Therefore, this appearance illustrated that the combined treatment of ultrasound and plasma protein treatment promoted the elasticity and viscosity changes in the composite protein.

4. Conclusion

Ultrasound assisted plasma protein treatment could promote the formation of covalent cross-links based on disulfide bonds in MP. This process increased the apparent viscosity and structural strength of the composite protein system. The spatial structure of the composite protein system was altered following by UPP treatment. Meanwhile, both average particle size and loss tangent were significantly reduced. These results indicated that UPP treatment enhanced the stability and adhesive properties of MP solutions. Collectively, this study elucidated the mechanism behind the positive influence of plasma protein on improving restructured chicken patties.

5. Consent from

This experiment is not involved animal experiments or sensory experiments.

CRediT authorship contribution statement

Ye Zou: Data curation, Formal analysis, Writing – original draft. **Lingjuan Wang:** Data curation, Formal analysis, Writing – original draft. **Xiaowen Wang:** Writing – review & editing. **Yibo Lan:** Investigation, Project administration. **Jingjing Ma:** Methodology, Investigation, Visualization, Writing – review & editing. **Jing Yang:** Project administration. **Weimin Xu:** Resources, Investigation. **Qi Shen:** Resources, Investigation, Writing – review & editing. **Daoying Wang:** Resources, Investigation.

Declaration of competing interest

The authors declare that they have no known competing financial interests or personal relationships that could have appeared to influence the work reported in this paper.

Acknowledgments

This study was supported by the China agriculture research system (CARS-41), Jiangsu Agriculture Science and Technology Innovation Fund (CX(24)1020), National Key Research and Development Program of China (2022YFD2100500) and Shandong Province Science and Technology based Small and Medium sized Enterprises Innovation Capability Enhancement Project (2023TSGC0367).

References

[1] P. Vahmani, E.N. Ponnampalam, J. Kraft, C. Mapiye, E.N. Bermingham, P. J. Watkins, et al., Bioactivity and health effects of ruminant meat lipids, Meat Sci. 165 (2020) e108114, https://doi.org/10.1016/j.meatsci.2020.108114.
[2] A. Dursun, Z. Güler, Colour and pigment in raw ground meat incorporated crushed garlic during the refrigerated storage: their relationship to lipolytic and volatilomic changes, Food Chem. 419 (2023) e136042, https://doi.org/10.1016/j.foodchem.2023.136042.
[3] B.M. Naveena, A.R. Sen, M. Muthukumar, Y. Babji, N. Kondaiah, Effects of salt and ammonium hydroxide on the quality of ground buffalo meat, Meat Sci. 87 (2011) 315–320, https://doi.org/10.1016/j.meatsci.2010.11.004.
[4] E. Fotou, V. Moulasioti, G.A. Papadopoulos, D. Kyriakou, M.E. Boti, et al., Effect of farming system type on broilers' antioxidant status, performance, and carcass traits: an industrial-scale production study, Sustainability 16 (2024) 4782, https://doi.org/10.3390/su16114782.
[5] Y. Zou, H. Yang, P.P. Li, M.H. Zhang, X.X. Zhang, W.M. Xu, et al., Effect of different time of ultrasound treatment on physicochemical, thermal, and antioxidant properties of chicken plasma protein, Poultry Sci. 98 (2019) 1925–1933, https://doi.org/10.3382/ps/pey502.
[6] G.H. Lu, T.C. Chen, Application of egg white and plasma powders as muscle food binding agents, J. Food Eng. 42 (1999) 147–151, https://doi.org/10.1016/S0260-8774(99)00112-0.
[7] S. Hurtado, E. Saguer, M. Toldrà, D. Parés, C. Carretero, Porcine plasma as polyphosphate and caseinate replacer in frankfurters (Article), Meat Sci. 90 (2012) 624–628, https://doi.org/10.1016/j.meatsci.2011.10.004.
[8] D.C. Kang, W.A. Zhang, J.M. Lorenzo, X. Chen, Structural and functional modification of food proteins by high power ultrasound and its application in meat processing, Crit. Rev. Food Sci. 61 (2021) 1914–1933, https://doi.org/10.1080/10408398.2020.1767538.
[9] G. Xiong, X. Fu, D. Pan, J. Qi, X. Xu, X. Jiang, Influence of ultrasound-assisted sodium bicarbonate marination on the curing efficiency of chicken breast meat, Ultrason. Sonochem. 60 (2020) e104808, https://doi.org/10.1016/j.ultsonch.2019.104808.
[10] A. Asghar, K. Samejima, T. Yasui, Functionality of muscle proteins in gelation mechanisms of structured meat products, Crit. Rev. Food Sci. 22 (1985) 27–106, https://doi.org/10.1080/10408398509527408.
[11] K. Li, L. Fu, Y.Y. Zhao, S.W. Xue, P. Wang, X.L. Xu, et al., Use of high-intensity ultrasound to improve emulsifying properties of chicken G protein and enhance the rheological properties and stability of the emulsion, Food Hydrocolloid. 98 (2020) e105275, https://doi.org/10.1016/j.foodhyd.2019.105275.
[12] Y. Sun, L. Ma, Y. Fu, H.J. Dai, Y.H. Zhang, The improvement of gel and physicochemical properties of porcine myosin under low salt concentrations by pulsed ultrasound treatment and its mechanism, Food Res. Int. 141 (2021) e110056, https://doi.org/10.1016/j.foodres.2020.110056.
[13] L.J. Wang, X.W. Wang, X.J. Qin, Z. Wang, Y. Zou, D.Y. Wang, et al., Restructured ground chicken quality study by ultrasound combined with plasma protein treatment, Food G. 56 (2023) e103289, https://doi.org/10.1016/j.fbio.2023.103289.
[14] S. Jiang, M. Zhang, H. Liu, Q. Li, D. Xue, Y. Nian, et al., Ultrasound treatment can increase digestibility of myofibrillar protein of pork with modified atmosphere packaging, Food Chem. 377 (2022) e131811, https://doi.org/10.1016/j.foodchem.2021.131811.
[15] H. Li, Y. Hu, X. Zhao, W. Wan, X. Du, B. Kong, et al., Effects of different ultrasound powers on the structure and stability of protein from sea cucumber gonad (Article), LWT 137 (2021) e110403, https://doi.org/10.1016/j.lwt.2020.110403.
[16] J.H. Chen, X. Zhang, M.Y. Fu, X. Chen, B.A. Pius, X.L. Xu, Ultrasound-assisted covalent reaction of myofibrillar protein: the improvement of functional properties and its potential mechanism, Ultrason. Sonochem. 76 (2021) e105652, https://doi.org/10.1016/j.ultsonch.2021.105652.
[17] X. Zhao, J. Qi, C. Fan, B. Wang, C. Yang, D. Liu, Ultrasound treatment enhanced the ability of the porcine myofibrillar protein to bind furan compounds: investigation of underlying mechanisms, Food Chem. 384 (2022) e132472, https://doi.org/10.1016/j.foodchem.2022.132472.
[18] Y.F. Gao, S.C. Wang, H.Y. Liu, Y.Y. Gu, J. Zhu, Design and characterization of low salt myofibrillar protein-sugar beet pectin double-crosslinked gels pretreated by ultrasound and G glucomannan: Conformational and gelling properties, Food Hydrocolloid. 141 (2023) e108717, https://doi.org/10.1016/j.foodhyd.2023.108717.
[19] J. Jiang, Z.P. Zhang, J. Zhao, Y.F. Liu, The effect of non-covalent interaction of chlorogenic acid with whey protein and casein on physicochemical and radical-scavenging activity of protein digests, Food Chem. 268 (2018) 334–341, https://doi.org/10.1016/j.foodchem.2018.06.015.
[20] K. Candogan, E.G. Altuntas, N. Igci, Authentication and quality assessment of meat products by Fourier-transform infrared (FTIR) spectroscopy, Food Eng. Rev. 13 (2021) 66–91, https://doi.org/10.1007/s12393-020-09251-y.
[21] Y.G. Cao, Z.R. Li, B.L. Li, X. Fan, M.M. Liu, J. Zhao, Mitigation of oxidation-induced loss of G protein gelling potential by the combination of pyrophosphate and L-lysine, G-Food Sci. Technol. 157 (2022) e113068, https://doi.org/10.1016/j.lwt.2022.113068.
[22] A. Amiri, P. Sharifian, N. Soltanizadeh, Application of ultrasound treatment for improving the physicochemical, functional and rheological properties of myofibrillar proteins, Int. J. Biol. Macromol. 111 (2018) 139–147, https://doi.org/10.1016/j.ijbiomac.2017.12.167.
[23] X. Du, M.N. Zhao, N. Pan, S.P. Wang, X.F. Xia, D.J. Zhang, Tracking aggregation behaviour and gel properties induced by structural alterations in myofibrillar

protein in mirror carp (Cyprinus carpio) under the synergistic effects of pH and heating, Food Chem. 362 (2021) e130222, https://doi.org/10.1016/j.foodchem.2021.130222.
[24] S. Esteghlal, H.H. Gahruie, M. Niakousari, F.J. Barba, A.E. Bekhit, K. Mallikarjunan, et al., Bridging the knowledge gap for the impact of non-thermal processing on proteins and amino acids, Foods 8 (2019) e262, https://doi.org/10.3390/foods8070262.
[25] M. Mishyna, J.J.I. Martinez, J.S. Chen, M. Davidovich-Pinhas, O. Benjamin, Heat-induced aggregation and gelation of proteins from edible honey bee brood (Apis mellifera) as a function of temperature and pH, Food Hydrocolloid. 91 (2019) 117–126, https://doi.org/10.1016/j.foodhyd.2019.01.017.
[26] F. Geng, Y.X. Xie, Y. Wang, J.Q. Wang, Depolymerization of chicken egg yolk granules induced by high-intensity ultrasound, Food Chem. 354 (2021) e129580, https://doi.org/10.1016/j.foodchem.2021.129580.
[27] Q. Liu, Q. Chen, B. Kong, J. Han, X. He, The influence of superchilling and cryoprotectants on protein oxidation and structural changes in the myofibrillar proteins of common carp (Cyprinus carpio) surimi (Article), LWT – Food Sci Technol. 57 (2014) 603–611, https://doi.org/10.1016/j.lwt.2014.02.023.
[28] J.H. Chen, X. Zhang, S.W. Xue, X.L. Xu, Effects of ultrasound frequency mode on myofibrillar protein structure and emulsifying properties, Int. J. Biol. Macromol. 163 (2020) 1768–1779, https://doi.org/10.1016/j.ijbiomac.2020.09.114.
[29] I. Gülseren, D. Güzey, B.D. Bruce, J. Weiss, Structural and functional changes in ultrasonicated bovine serum albumin solutions, Ultrason. Sonochem. 14 (2007) 173–183, https://doi.org/10.1016/j.ultsonch.2005.07.006.
[30] D.C. Kang, Y.H. Zou, Y.P. Cheng, L.J. Xing, G.H. Zhou, W.G. Zhang, Effects of power ultrasound on oxidation and structure of beef proteins during curing processing, Ultrason. Sonochem. 33 (2016) 47–53, https://doi.org/10.1016/j.ultsonch.2016.04.024.
[31] Y. Zou, F. Lu, B. Yang, J. Ma, J. Yang, C. Li, et al., Effect of ultrasound assisted G G treatment on properties of chicken plasma protein gelation, Ultrason. Sonochem. 80 (2021) e105821, https://doi.org/10.1016/j.ultsonch.2021.105821.
[32] L.P. Xu, W.Q. Yan, M. Zhang, X. Hong, Y.F. Liu, J.W. Li, Application of ultrasound in stabilizing of Antarctic krill oil by modified chickpea protein isolate and ginseng saponin, LWT – Food Sci Technol. 149 (2021) e111803, https://doi.org/10.1016/j.lwt.2021.111803.
[33] F. Ekezie, J. Cheng, D. Sun, Effects of atmospheric pressure plasma jet on the conformation and physicochemical properties of myofibrillar proteins from king prawn (Litopenaeus vannamei) (Article), Food Chem. 276 (2019) 147–156, https://doi.org/10.1016/j.foodchem.2018.09.113.
[34] C. Fernández-Avila, R. Escriu, A.J. Trujillo, Ultra-High Pressure Homogenization enhances physicochemical properties of soy protein isolate-stabilized emulsions, Food Res. Int. 75 (2015) 357–366, https://doi.org/10.1016/j.foodres.2015.05.026.
[35] X.H. Tong, J. Cao, T. Tian, B. Lyu, L.M. Miao, Z.T. Lian, et al., Changes in structure, rheological property and antioxidant activity of soy protein isolate fibrils by ultrasound pretreatment and EGCG, Food Hydrocolloid. 122 (2022) e107084, https://doi.org/10.1016/j.foodhyd.2021.107084.
[36] X.Q. Chen, X.Y. Chu, X. Li, F.L. Cao, Q.R. Guo, J.H. Wang, Non-thermal plasma modulation of the interaction between whey protein isolate and ginsenoside Rg1 to improve the rheological and oxidative properties of emulsion, Food Res. Int. 165 (2023) e112548, https://doi.org/10.1016/j.foodres.2023.112548.
[37] L. Zhang, F. Zhang, X. Wang, Effects of hydrolyzed wheat gluten on the properties of high-temperature (≥100°C) treated surimi gels (Article), Food Hydrocolloid. 45 (2015) 196–202, https://doi.org/10.1016/j.foodhyd.2014.11.016.
[38] H.F. Wang, P.Y. Wang, Q. Shen, H.J. Yang, H.J. Xie, M. Huang, et al., Insight into the effect of ultrasound treatment on the rheological properties of myofibrillar proteins based on the changes in their tertiary structure, Food Res. Int. 157 (2022) e111136, https://doi.org/10.1016/j.foodres.2022.111136.
[39] Y.M. Pan, Q.X. Sun, Y. Liu, S. Wei, Q.Y. Xia, O. Zheng, et al., The relationship between rheological and textural properties of shrimp surimi adding starch and 3D printability based on principal component analysis, Food Sci. Nutr. 9 (2021) 2985–2999, https://doi.org/10.1002/fsn3.2257.
[40] Z.L. Zhao, Q. Wang, B.W. Yan, W.H. Gao, X.D. Jiao, J.L. Huang, et al., Synergistic effect of microwave 3D print and transglutaminase on the self-gelation of surimi during printing, Innov. Food Sci. Emerg. Technol. 67 (2021) e102546, https://doi.org/10.1016/j.ifset.2020.102546.